Journal of Molecular Structure 1191 (2019) 118–128

Contents lists available at ScienceDirect

Journal of Molecular Structure

journal homepage: http://www.elsevier.com/locate/molstruc

Spectroscopic exploration of binding of new imidazolium-based palladium(II) saldach complexes with CT-DNA as anticancer agents against HER2/neu overexpression

Mohammad Y. Alfaifi [a], Serag Eldin I. Elbehairi [a], Hani S. Hafez [b], Reda F.M. Elshaarawy [c, *]

[a] Biology Department, Faculty of Science, King Khalid University, 9004, Abha, Saudi Arabia
[b] Faculty of Science, Zoology Department, Suez University, 43533, Suez, Egypt
[c] Faculty of Science, Chemistry Department, Suez University, 43533, Suez, Egypt

ARTICLE INFO

Article history:
Received 18 February 2019
Received in revised form
10 April 2019
Accepted 27 April 2019
Available online 29 April 2019

Keywords:
Imidazolium motifs
Pd(II) saldach
Cytotoxicity
CT-DNA interaction-HER2/neu
Apoptosis

ABSTRACT

The *HER2/neu* has shown a potential role in the choice of active chemotherapy for breast tumors because of its prognostic relevance and putative role in predicting drug resistance. Moreover, suppressing DNA replication has become an attractive strategy for treating cancer patients. In this attempt, the present study aimed to prepare new series of *bis*-imidazolium-based saldach {$H_2(Et)_2$saldach (^{n}Bu-Im$^+$-X$^-$)$_2$} and their *cis*-Pd(II) complexes (saldach = *N,N′*-bis-(salicylidene)-*R,R*-1,2-diaminocyclohexane; X = Cl, PF_6, BF_4) as anticancer agents. The *in vitro* cytotoxicity activity of new *cis*-Pd(II) complexes against human breast adenocarcinoma cell lines (MCF-7) revealed higher growth-inhibitory effect than the native ligands. They induced a significant decrease for the protein HER2/neu expression with $p < 0.05$ and tumor necrosis factor (TNF-α) ($p < 0.05$), while the tumor suppressor protein P53 was expressed in a highly significant upregulation $p < 0.01$. Moreover, complex **5**a was the most potent active compound ($IC_{50} = 8.5 \pm 0.2$ μM) in inhibition of cell proliferation. Additionally, *in vitro* studies of Pd(II) complex (**5a)** using UV–Vis spectroscopy and binding affinity toward the calf thymus (CT) DNA) showed a combination of covalent, intercalation, hydrogen bonding interactions through formation of (CT-DNA).

1. Introduction

Human epidermal receptor 2 (HER2) gene [1] overexpression is deemed to be one of the proteins that often recognized in various numbers of primary tumors and their contribution to the transformation process to tumorigenesis [2]. Approximately, 27.5 ± 2.5% of patients with breast cancer overexpresses HER2 [3], leading to restricted clinical outcome in patients [4] HER-2/neu−overexpression was demonstrated to boost proliferative, pro-survival, and [5] metastatic signals within the breast cancer cells [6] and carcinomas development [7]. It plays an important role in the amendment of cellular response to cytotoxic tumor necrosis factor (TNF) [8]. HER-2/neu−over-expressing and transfected cells are resistant to the cytotoxic action of TNF [9].

The clinical difficulties of platinum (Pt)-based anticancer drugs [10] such as narrow-spectrum, intrinsic toxicity, and drug resistance [11] have promoted scientists for expedition of another new non-Pt metal-based anti-cancer compounds [12]. Although no non-Pt metal anticancer agents has been recommended for today cancer chemotherapy, extensive improvement has been carried out in the improving of such drugs [13].

Moreover, a great effort has been devoted for exploring of new Pd(II) complexes expressing significant wide range as anticancer fighting agents against diverse cancer cell lines [14], and lower side effects as compared with cisplatin [15], usually applied as a non-platinum chemotherapeutic in tumor therapy [16]. As a remarkable character of metal-based anti-cancer agents, Pd(II) complexes exhibited lower kidney toxicity than cisplatin [13]. Two main distinctions between Pt and Pd complexes are desirable to be mentioned; (i) Pd(II) complexes exhibited preferable solubility in relation to Pt(II) complexes, and (ii) the ligand-exchange and aquation reactions for Pd(II) complexes rates are ~10^5 times faster than the Pt(II) analogus [17]. Interestingly, a significant link has been noticed between the anti-cancer action of the Pd(II) complexes and their lipophilicity/solubility [18].

* Corresponding author.
E-mail addresses: reel-001@hhu.de, reda.elshaarawy@suezuniv.edu.eg (R.F.M. Elshaarawy).

https://doi.org/10.1016/j.molstruc.2019.04.119
0022-2860/

Noteworthy, metallosalen and metallo Schiff bases are often thought to be of the most studied classes of chemical nucleases which can effectively interact with, deteriorate and cleave damage nucleic acids [19] through the oxidative alkylation of DNA bases [20]. Some recent studies revealed that Pd(II) Schiff bases complexes can perform as anti-breast cancer agents *via* playing several possible roles in cancer cell apoptosis such as fragmentation probes for cleavage of CT-DNA [16,21], fluorescent probes for protein and/or nuclear and components [22], DNA photo cleavage probes [23], as an ribonucleotide reductase inhibitor inducing genetic material damage [24] or as catalytic poisons of human topoisomerase IIa [22]. Also, they exhibit a strong binding affinity with the transporting proteins [25].

The amazing pharmacological aspects of 1,3-dialkylimidazolium salts [26] make them interesting candidates for treatment in chemotherapy owing to their capacity to provoke diverse biological responses upon interaction with different biotargets.

Inspired by the previous facts and our ongoing interest in exploring of new, vigorous, selective and safe chemotherapeutic candidates [27], we reported in this study the synthesis and the anti-cancer action of a unique series of Pd(II)-saldach complexes anchored imidazolium motifs (Fig. 1), where saldach is *N,N′*-bis-(salicylidene)-*R,R*-1,2-diaminocyclo-hexane, against cultured human breast cancer cells (MCF-7).

2. Experimental

2.1. Materials and methods

Details of instrumentation, chemical suppliers and reagents for the *in vitro* experiments are given in the Electronic Supplementary Information (ESI†).

2.2. Preparation of key starting materials (1–3)

The key starting materials, materials (*R,R*)-1,2-diaminocyclohexane (*R,R*-dach), 3-ethylsalicylaldehyde (**1**), 3-ethyl-5-chloromethyl-2-hydroxybenzaldehyde (**2**) and 3-(3-(ethyl)-5-formyl-4-hydroxybenzyl)-1-butyl- imidazolium chloride, hexafluorophosphate and tetrafluoroborate, (Et)sal(^{n}Bu-Im$^+$-X$^-$) (**3**a-c) were prepared following the procedures reported in ESI†.

2.3. General method for preparation of *R,R*-{H_2(Et)$_2$saldach(^{n}Bu-Im$^+$-X$^-$)$_2$} (4a-c)

An ethanolic solution of *R,R*-dach (0.23 g, 2.0 mmol/10 mL) was prepared in a Schlenk tube and added with vigorous stirring to a solution of imidazolium salt (Et)sal(^{n}Bu-Im$^+$-X$^-$) (**3**a-c) (4.0 mmol/20 mL EtOH) into a 100 mL Schlenk flask under N_2 atmosphere. Then the mixture was refluxed with stirring under the same atmosphere for 3 h. Thereafter, the solvent was removed under reduced pressure to give a very viscous residue which was solidified by the addition of ethyl acetate (AcOEt) and keeping in the refrigerator overnight to afford the desired products (**4a-c**). AcOEt was decanted off, and the isolated crude products were purified by washing with Et_2O (3 × 25 mL), under ultrasonic irradiation, followed by MeOH/Et_2O mixture (1:2) to remove the unreacted materials. Then the residue was redissolved in a minimum amount of EtOH and repreciptated gradually by addition of EtOAc through (~15 min) to yield pure products which were gathered by filtration and vacuum-dried overnight at 40 °C.

2.3.1. *N,N′-Bis[3-ethyl-5-((1-^{n}butylimidazol-3-ium)methylene)-salicylidene)-R,R-1,2-cyclohexane diamine dichloride (4a)*

Yellowish orange powder, (89%); mp 65–66 °C. FT-IR (KBr, cm^{-1}): 3445 (m, br), 3058 (m, sh), 2919 (m, sh) 1629 (vs, sh, $\nu_{(C=N)}$), 1538, 1460, 1383 (s, sh), 1276 (s, sh), 1159 (s, sh), 770 (m, sh), 645 (m, sh). ^{1}H NMR (200 MHz, $CDCl_3$) δ (ppm): 10.61 (s, 2H), 8.21 (s, 2H), 7.92 (d, J = 2.01 Hz, 2H), 7.64 (d, J = 1.98 Hz, 2H), 7.44 (d, J = 1.59 Hz, 2H), 7.22 (d, J = 1.85 Hz, 2H), 5.64 (s, 4H), 4.26 (t, J = 7.0 Hz, 4H), 3.34 (m, 2H), 2.72 (q, J = 7.5 Hz, 4H), 1.87 (m, 4H), 1.50 (m, 4H), 1.26 (t, J = 7.5 Hz, 6H), 1.21 (m, 4H), 0.91 (t, J = 7.3 Hz, 3H). ^{13}C NMR (125 MHz, $CDCl_3$) δ (ppm): 164.65, 149.28, 136.27, 163.33, 125.80, 123.08, 122.91, 122.71, 119.93, 117.82, 56.66, 49.06, 39.41, 34.60, 31.61, 27.89, 25.24, 23.39, 22.80, 19.16, 13.62. ESI MS: *m/z* 687.4 and 326.1 ([$C_{40}H_{56}ClN_6O_2$]$^+$ and [$C_{40}H_{56}N_6O_2$]$^{2+}$, [M − Cl$^-$]$^+$ and [M − 2Cl$^-$]$^{2+}$, respectively). Anal. Calcd. for $C_{40}H_{56}Cl_2N_6O_2$ (M = 723.82): C, 66.37; H, 7.80; N, 11.61; Found: C, 65.71; H, 7.83; N, 11.49.

2.3.2. *N,N′-Bis[3-ethyl-5-((1-^{n}butylimidazol-3-ium)methylene)-salicylidene)-R,R-1,2-cyclohex- anediamine bis-(hexafluorophosphate) (4b)*

Yellow powder, (86%); mp 93–94 °C. FT-IR (KBr, cm^{-1}): 3436 (m, br), 3150 (m, sh), 2938 (m, sh), 1626 (vs, sh), 1539, 1466, 1389 (s, sh), 1273 (s, sh), 1160 (s, sh), 838 (vs, sh), 774 (m, sh), 676 (m, sh), 557 (s, sh). ^{1}H NMR (200 MHz, DMSO-d_6) δ (ppm): 9.20 (s, 2H), 8.52 (s, 2H), 7.65 (d, J = 2.07 Hz, 2H), 7.61 (d, J = 1.99 Hz, 2H), 7.33 (s, 2H), 7.21 (s, 2H), 5.79 (s, 4H), 4.18 (t, J = 6.9 Hz, 4H), 3.38 (m, 2H), 2.74 (q, J = 7.3 Hz, 4H), 1.81 (m, 4H), 1.56 (m, 4H), 1.27 (t, J = 7.3 Hz, 6H), 1.22 (M, 4H), 0.87 (t, J = 7.4 Hz, 3H). ^{13}C NMR (125 MHz, DMSO-d_6) δ (ppm): 164.88, 151.32, 136.21, 133.13, 132.40, 125.02, 123.06, 122.69, 118.73, 117.62, 71.66, 65.28, 49.02, 36.13, 32.97, 31.61, 31.04, 24.05, 19.16, 16.53, 12.61. ^{31}P NMR (202 MHz, DMSO-d_6): −142.96 ppm (septet, $^2J_{PF}$ = 711.23 Hz). ^{19}F NMR (470 MHz, DMSO-d_6): −70.59 ppm (doublet, $^1J_{FP}$ = 715.68 Hz). HR-ESI-MS: 797.4176 and 326.1896 ([$C_{40}H_{56}F_6N_6O_2P$]$^+$ and [$C_{40}H_{56}N_6O_2$]$^{2+}$, [M − PF_6^-]$^+$ and [M − 2PF_6^-]$^{2+}$, respectively). Anal. Calcd. for $C_{40}H_{56}F_{12}N_6O_2P_2$ (M = 942.84): C, 50.96; H, 5.99; N, 8.91; Found: C, 50.72; H, 6.03; N, 8.85.

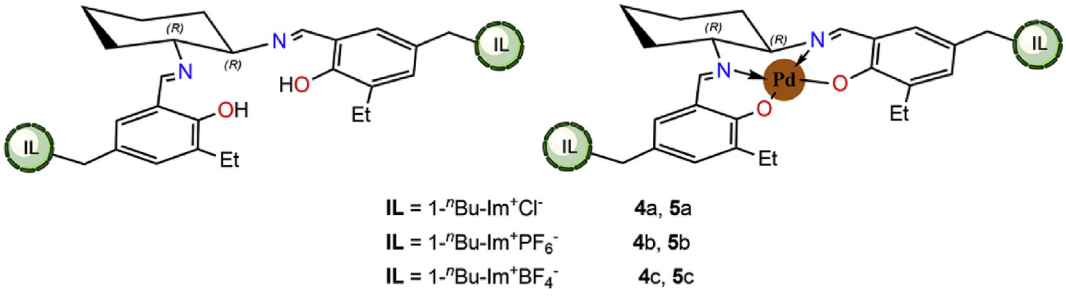

Fig. 1. Saldach-bis-imidazolium salts *R,R*-{H_2(Et)$_2$saldach(^{n}Bu-Im$^+$-X$^-$)$_2$}and Pd(II) complexes [Pd(II){(Et)$_2$saldach(^{n}Bu-Im$^+$-X$^-$)$_2$}] used in our work.

2.3.3. N,N′-Bis[3-ethyl-5-((1-^{n}butylimidazol-3-ium)methylene)-salicylidene)-R,R-1,2-cyclohex- anediamine bis-(tetrafluoroborate) (4c)

Faint yellow powder, (87%); mp 77–78 °C. FT-IR (KBr, cm^{-1}): 3426 (m, br, $\nu_{(O-H)}$), 3098 (m, sh), 2936 (m, sh), 1623 (vs, sh), 1538, 1463, 1389 (s, sh), 1281 (s, sh), 1158 (s, sh), 1060 (vs, sh), 865 (m, sh), 771 (m, sh). ^{1}H NMR (200 MHz, DMSO-d_6) δ (ppm): 9.22 (s, 2H), 8.43 (s, 2H), 7.81 (d, J = 2.05 Hz, 2H), 7.73 (d, J = 2.05 Hz), 7.37 (d, J = 1.86 Hz, 2H), 7.25 (d, J = 2.01 Hz, 2H), 5.82 (s, 4H), 4.20 (t, J = 7.1 Hz, 4H), 3.41 (m, 2H), 2.73 (q, J = 7.3 Hz, 4H), 1.79 (m, 4H), 1.52 (m, 4H), 1.28 (t, J = 7.2 Hz, 6H), 1.19 (m, 4H), 0.87 (t, J = 6.0 Hz, 3H). ^{13}C NMR (125 MHz, DMSO-d_6) δ (ppm): 165.58, 151.03, 138.85, 138.02, 133.35, 129.94, 129.52, 123.91, 122.88, 71.24, 55.89, 48.52, 34.31, 30.87, 29.76, 28.41, 25.94, 23.68, 22.34, 13.86. ^{19}F NMR (470 MHz, DMSO-d_6): 148.72 ppm (singlet). ESI-MS: 739.4 and 326.0 ($[C_{40}H_{56}BF_4N_6O_2]^+$ and $[C_{40}H_{56}N_6O_2]^{2+}$, $[M - BF_4^-]^+$ and $[M - 2\ BF_4^-]^{2+}$, respectively). Anal. Calcd. for $C_{40}H_{56}B_2F_8N_6O_2$ (M = 826.52): C, 58.13; H, 6.83; N, 10.17; Found: C, 57.99; H, 6.86; N, 10.05.

2.4. Preparation of {Pd(II)(Et)$_2$saldach(^{n}Bu-Im^{+}-X^{-})$_2$} complexes (5a-c)

A solution of palladium(II) chloride (0.126 g, 1 mmol/5 mL EtOH) was added dropwise to an ethanolic solution (10 mL) containing the free ligand (**4**a-c) (1 mmol) and 1 mL of conc HCl. Thereafter, the reaction mixture was refluxed under constant stiring for 6 h. Then the solvent was evaporated under vacuum to leave an oily residue, which was solidified by addtion of petroleum ether (40–60) and keeping overnight in a refrigerator. The isolated products were filtered off and washed with ice-cold mixed-solvent of MeOH/Et_2O (1 : 2) (3 × 3 mL) to yield Pd(II) saldach complexes (**5**a–c).

2.4.1. R,R-[[2,2`-][(1,2-cyclohexanediyl)-bis(nitrilomethylidyne)]-bis[4-((1-^{n}butylimidaz- olium)-methylene-6-(ethyl-phenolato)]-[N,N',O,O'] palladium(II) dichloride (5a)

Dark yellow powder (68%). FT-IR (KBr, cm^{-1}): 1633 (vs, sh), 1267 (s, sh), 615 (m, sh), 496 (w, br). ^{1}H NMR (200 MHz, $CDCl_3$) δ (ppm): 8.37 (s, 2H), 7.75 (d, J = 2.00 Hz, 2H), 7.71 (d, J = 1.99 Hz, 2H), 7.39 (d, J = 1.63 Hz, 2H), 7.24 (d, J = 1.85 Hz, 2H), 5.83 (s, 4H), 4.18 (t, J = 7.0 Hz, 4H), 3.35 (m, 2H), 2.72 (q, J = 7.3 Hz, 4H), 1.77 (m, 4H), 1.50 (m, 4H), 1.26 (t, J = 7.5 Hz, 6H), 1.19 (m, 4H), 0.91 (t, J = 7.1 Hz, 3H). ESI MS: m/z 792.6 and 378.3 ($[C_{40}H_{54}ClN_6O_2Pd]^+$ and $[C_{40}H_{54}N_6O_2Pd]^{2+}$, $[M - Cl^-]^+$ and $[M - 2Cl^-]^{2+}$, respectively). Anal. Calcd. for $C_{40}H_{54}Cl_2N_6O_2Pd$ (M = 828.22): C, 58.01; H, 6.57; N, 10.15; Found: C, 57.96; H, 6.63; N, 10.09.

2.4.2. R,R-[[2,2`-][(1,2-cyclohexanediyl)-bis(nitrilomethylidyne)]-bis[4-((1-nbutylimidaz-olium)-methylene-6-(ethyl-phenolato)]-[N,N',O,O'] palladium(II) bis-(hexafluoro-phosphate) (5b)

Faint brown powder (67%). FT-IR (KBr, cm^{-1}): 1633 (vs, sh), 1266 (s, sh), 840 (vs, sh), 612 (m, sh), 559 (m, sh), 492 (w, br). ^{1}H NMR (200 MHz, DMSO-d_6) δ (ppm): 8.36 (s, 2H), 7.64 (d, J = 2.03 Hz, 2H), 7.59 (d, J = 2.00 Hz, 2H), 7.36 (s, 2H), 7.23 (d, J = 1.86 Hz, 2H), 5.28 (s, 4H), 4.18 (t, J = 7.0 Hz, 4H), 3.37 (m, 2H), 2.73 (q, J = 7.1 Hz, 4H), 1.80 (m, 4H), 1.53 (m, 4H), 1.28 (t, J = 7.4 Hz, 6H), 1.18 (m, 4H), 0.89 (t, J = 7.0 Hz, 3H). ^{31}P NMR (202 MHz, DMSO-d_6): −142.96 ppm (septet, $^{2}J_{PF}$ = 711.23 Hz). ^{19}F NMR (470 MHz, DMSO-d_6): −70.59 ppm (doublet, $^{1}J_{FP}$ = 715.68 Hz). ESI MS: m/z 901.4 and 378.1 ($[C_{40}H_{54}F_4N_6O_2PPd]^+$ and $[C_{40}H_{54}N_6O_2Pd]^{2+}$, $[M - PF_6^-]^+$ and $[M - 2PF_6^-]^{2+}$, respectively). Anal. Calcd. for $C_{40}H_{54}F_{12}N_6O_2P_2Pd$ (M = 1047.24): C, 45.88; H, 5.20; N, 8.02; Found: C, 45.63; H, 5.22; N, 7.98.

2.4.3. R,R-[[2,2`-][(1,2-cyclohexanediyl)-bis(nitrilomethylidyne)]-bis[4-((1-nbutylimidaz-olium)-methylene-6-(ethyl-phenolato)]-[N,N',O,O'] palladium(II) bis-(tetrafluoro-borate) (5c)

Reddish-brown powder (62%). FT-IR (KBr, cm^{-1}): 1634 (vs, sh, $\nu_{(C=N)}$), 1267 (s, sh), 1058 (vs, sh), 615(m, sh), 493 (w, br). ^{1}H NMR (200 MHz, DMSO-d_6) δ (ppm): 8.35 (s, 2H), 7.80 (d, J = 2.01 Hz, 2H), 7.74 (d, J = 2.01 Hz), 7.36 (d, J = 1.89 Hz, 2H), 7.26 (d, J = 2.00 Hz, 2H), 5.83 (s, 4H), 4.21 (t, J = 7.0 Hz, 4H), 3.42 (m, 2H), 2.73 (q, J = 7.1 Hz, 4H), 1.81 (m, 4H), 1.53 (m, 4H), 1.27 (t, J = 7.1 Hz, 6H), 1.16 (m, 4H), 0.87 (t, J = 6.3 Hz, 3H). ^{19}F NMR (470 MHz, DMSO-d_6): 148.72 ppm (singlet). ESI-MS: 844.1 and 378.1 ($[C_{40}H_{54}BF_4N_6O_2Pd]^+$ and $[C_{40}H_{54}N_6O_2Pd]^{2+}$, $[M - BF_4^-]^+$ and $[M - 2\ BF_4^-]^{2+}$, respectively). Anal. Calcd. for $C_{40}H_{54}B_2F_8N_6O_2Pd$ (M = 930.92): C, 51.61; 5.85; N, 9.03; Found: C, 51.47; H, 5.91; N, 8.94.

2.5. Stability of complexes under physiological conditions

The stability of Pd(II) complexes was investigated by recording UV–Vis spectroscopy for a solution (1×10^{-3} M) of complex in a DMSO/phosphate buffer of pH 7.4 in time intervals (t = 0 h, 1 week, 2 weeks) at 25 °C. Buffer solution was prepared by adding 70 mL 0.1 M aqueous NaOH solution to 0.1 M aqueous KH_2PO_4 solution. The pH of the obtained DMSO:PBS buffer was checked with the HANA instrument 8519 digital pH-meter.

2.6. In vitro anticancer (cytotoxicity)

2.6.1. Cell cultures

Human tumor cell lines MCF-7 (breast adenocarcinoma) have been acquired from the VACSERA Tissue Culture Unit, and cultured using RPMI-1640 media with and 10% FBS, 1% L-glutamine, HEPES buffer with the addition of 50 μg/mL gentamycin. Cells have been sustained at 37 °C in 5% CO_2. Toxicity has been measured according to the activity of cell morphology and cell viability. Control cells were treated with 0.5% DMSO.

2.6.2. Cytotoxic effect assay

Cytotoxicity effects of *R,R*-{H_2(Et)$_2$saldach(^{n}Bu-Im^{+}-X^{-})$_2$} (**4**a-c) and their Pd(II) complexes [Pd(II){(Et)$_2$saldach(^{n}Bu-Im^{+}-X^{-})$_2$}] (**5**a-c) were assessed by the *in-vitro* cytotoxicity assay according to the adopted methods instruction of the Regional Center for Mycology & Biotechnology, Egypt. In brief, 1×10^4 cells per well in 100 μL of growth medium were seeded in 96-well plates. Moreover, serial dilutions of the compounds have been added to the confluent cell mono layers plates (Falcon, NJ, USA) using a multichannel pipette; followed by incubation at 37 °C using humid 5% CO_2 incubator for 48 h plate wells have been divided into three wells for each sample concentration and control cells have been incubated with and without DMSO. Different sample concentrations were used as follows; 50, 25, 12.5, 6.25, 3.125, 1.56 μg for 24 h and continued incubation for time for 48 h. Finally, the viable cells yield was determined by a colorimetric method followed by the addition of crystal violet solution (1%) to each well for at least 30 min. The crystal violet stain excess has been detached using running water followed by addition of glacial acetic acid (30%) to all wells and mixed thoroughly by gently shaking to measure their absorbance using Micro plate reader (TECAN, Inc.) at wavelength of 490 nm. Additionally, the cytotoxic effects of the used compounds have been measured through comparison of the treated samples with the control cell [28].

2.7. DNA-binding study

The DNA-binding studies for the free ligand (**4**a) and its Pd(II)

complex have been carried out in a 10 mM Tris buffer/50 mM NaCl at pH 7.2. A stock solution of **4**a/**5**a (1 mM) was prepared in a milli-Q water containing DMSO ([DMSO] not more than 0.1% v/v). Constant concentrations of **4**a/**5**a (6×10^{-5} M/1×10^{-4} M) with different DNA concentrations varying from 0 to 5 mM have been used for the UV–Vis absorption titration in the rang of 200–600 nm.

The CT-DNA viscosity studies have been carried out carried out using a semimicro-viscometer held at 27 °C in a thermostatic water bath according to the earlier reported work [29].

2.8. Western blot analysis

The total protein has been extracted from the cultivated cells or frozen cancer tissue in an ice-cold lysis buffer pH 7.5 (50 mmol Tris–HCl, 150 mmol NaCl, 5 mmol EDTA, 1% Nonidet P-40 per litter) containing a protease inhibitor cocktail (SIGMA*FAST*™). 20 μg protein was gathered by a 12% SDS-PAGE and then transferred to a polyvinylidene difluoride (PVDF) membrane. After treatment with 5% nonfat milk in a PBS–Tween-20 (0.05%) (as a blocking solution) overnight at 4 °C, the membrane was then probed with the primary antibody specific to Hert2/neu (ErbB2/Her2 rabbit polyclonal) and β-actin (Novus Biologicals), followed by the HRP-conjugated secondary antibody. The enhanced chemiluminescence (ECL) from LUMIGEN Science has been used to visualize the antibody interaction. Bands were quantified by a calibrated imaging densitometer and analyzed by "Quantity One" software (Bio-Rad).

2.9. The enzyme-linked immunosorbent assay (ELISA)

ELISA analysis has been used to estimate the TNF-α and P53 expression levels in MCF-7 (breast adenocarcinoma) cell lines in 48-well plates. Phosphate buffered solution pH = 7.6 and 250 μL of serum-free DMEM have been used to rinse cultured cells. Concentrations of TNF-α has been calculated using TNF-α kit and P53 (ThermoFisher Scientific) according to the manufacturer's instructions. The induced cytotoxicity was calculated by using the following equation:

$$\text{Cell death rate } (\%) = \left(1 - \frac{OD_{sample}}{OD_{control}}\right) x\ 100\%$$

where the optical density (OD) values for the sample and cotrorl have been measured at a test wavelength of 570 nm, and a reference wavelength of 655 nm. $OD_{sample} = OD_{sample(570nm)} - OD_{sample(655nm)}$, and $OD_{control} = OD_{control(570nm)} - OD_{control(655nm)}$.

2.10. Statistical analyses

The data and mathematical calculation for the area under cell viability curves along with the group comparison was carried out by independent student's t-test using SPSS v17. P value of <0.05 was considered as the significant value.

3. Results and discussion

3.1. Synthesis protocol

The free bis-imidazolium salts bearing saldach scaffold (saldach = *N, N′*-bis-(salicylidene -*R,R*-1,2-diaminocyclohexane) have been prepared by the interaction of ethylsalicylaldehyde-butylimidazolium salts (**3**a-c) with *R,R*-1,2-diaminocyclohexane (*R,R*-dach) (Scheme 1) in a 2 : 1 M ratio an ethanolic solution under inert atmosphere using Schlenck technique. Intially, ethylsalicylaldehyde-butylimidazolium salts (**3**a-c) have been synthesized using 3-ethylsalicylaldehyde as a starting material based on multiple consecutive chemical strategies (*ortho*-formylation, chloromethylation, quarternization and anion metathesis) following a modified reported method [52]. Then, Schiff-base condensation of ethylsalicylaldehyde-butylimidazolium salts (**3**a-c) with (*R,R*-dach) offered the desired ligands (**4**a-c) which used as chelating agents for Pd(II) ions to prepare Pd(II) saldach complexes (**5**a-c).

The free ligands and their Pd(II) complexes were obtained in high yields. They were structurally characterized based upon microanalytical and spectral analysis, FTIR, UV–Vis, NMR (^{1}H, ^{13}C, ^{19}F, ^{31}P) as well as ESI-MS.

3.2. Microanalytical data and mass spectrometry

The free saldach ligands and their complexes were given satisfactorily elemental analyses, which are in full agreement with the proposed structural formulas for them (see the Experimental section).

The positive mode electron spray ionization (ESI) mass spectra of **4**a-b and Pd(II) complexes (**5**a-b) show dominant peaks for the singly and doubly charged cations as a result from the consecutive departure of anionic species (Cl^-, PF_6^- and BF_4^-) from the parent molecules.

3.3. Saldach ligands-Pd(II) ions binding profile and stability of complexes

The selected infrared spectral features of new ligands $\{H_2(Et)_2saldach(^nBuIm^+X^-)_2\}$ and their Pd(II) complexes $\{Pd(Et)_2saldach(^nBuIm^+X^-)_2\}$ demonstrate a successful formation of saldach ligands and their chelation to Pd(II) ions as revealed from the IR signatures along with their tentative assignments. Where the main IR spectral marker peaks noticed in the spectra of parent ligands at the regions of 3426–3445, 1626 ± 3 and 1277 ± 4 cm^{-1} assignable for the vibration of phenolic OH, azomethinic C=N and aryl-O groups, respectively, characteristic for the saldach structural motif. These stretches were either missed and/or fluctuated in spectra of Pd(II) complexes and consequently could be used as the informative spectral Pd(II)-saldach binding markers. For example, the losing of phenolic OH band along with a fluctuation of the intensity as well as negative energy-shift ($\Delta\nu = -(11 \pm 3)$ cm^{-1}) of aryl-O stretch (see Fig. 2) are indicative of the deprotonation phenolic OH group and ligation of the phenolate oxygen to Pd(II) ion. Furthermore, the characteristic azomethinic (H-C=N) stretch for the free saldach ligands is red-shifted by 5–10 cm^{-1}, in the spectra of complexes providing and evidence for the binding of the azomethinic nitrogen to Pd(II) ion.

Notably, Pd(II) complexes exhibit high stability under physiological conditions as evidenced by UV–Vis spectroscopy obtained for a 10^{-3} M solution of $\{Pd(Et)_2saldach(^nBu\text{-}Im^+\text{-}BF_4^-)_2\}$ (**5**b) in DMSO:PBS buffer (pH = 7.4), which did not reveal any significant change the spectrum of **5**b solution (Fig. S1, ESI†), as an indication for non-decomposition, of the complex with measurements over 2 weeks at room temperature.

3.4. Tautomeric scenario and H-bonding map in ligands analyzed by NMR

The relative populations of bis-imdazolium-saldach ligands (**4**a-c) tautomers in their deuterated solution could be easily estimated using NMR spectra. For example, $\{H_2(Et)_2saldach(^nBuIm^+\ Cl^-)_2\}$ (**4**a) has a very crowded ^{1}H NMR spectrum with strong coupling profile. This due to the co-existence of two set of proton signals assignable to the presence of a pair of tautomers in its deuterated solution with various populations. Meanwhile, the main

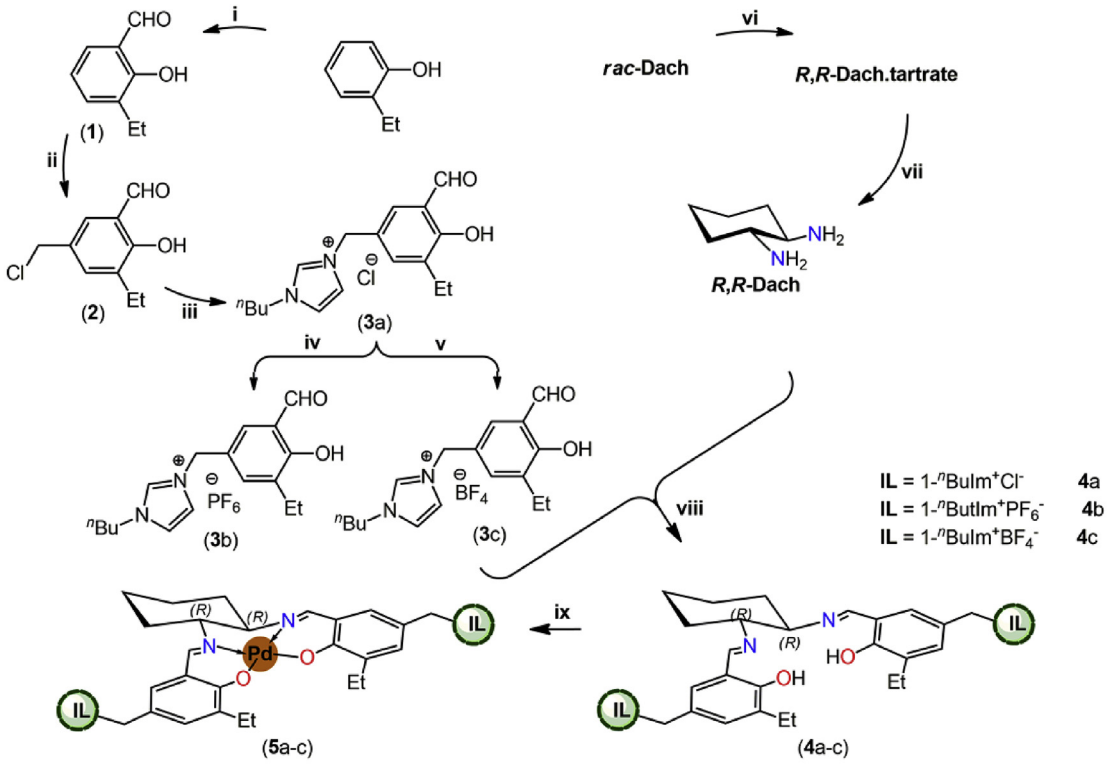

(i) Dry $MgCl_2$, $(CH_2O)_n$, Et_3N, ACN, stir, r.t; 2. HCl; (ii) CH_2O, $ZnCl_2$, HCl_{aq}, HCl_g, stirr, r.t; (iii) 1-^{n}Bu-Im, toluene, stir, 80 °C, N_2; (iv) 60 % HPF_6, milli-Q H_2O, stir, r.t., 3h; (v) $NaBF_4$, milli-Q H_2O, stir, r.t., 3h; (vi) L-(+)-tartaric acid, milli-Q H_2O, 100% AcOH, stir, 80 °C, 2h (vii) NaOH, dist. H2O, CH2Cl2, stir, 30 min, (viii) EtOH, reflux, stir, N_2; (ix) PdCl2, EtOH, stir, 50 °C, 8h.

Scheme 1. Synthesis protocol for ethylsalicylaldehyde-butylimidazolium salts (**3**a-c), $H_2(Et)_2$saldach(IL)$_2$ ligands (**4**a-c) and Pd(II) complexes (**5**a-b).

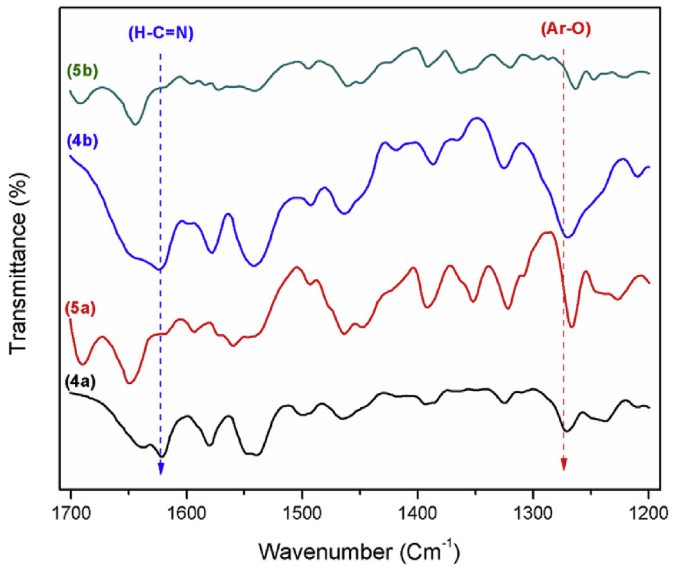

Fig. 2. Picked IR region (1700-1200 cm^{-1}) for an illustration of the fluctuation of azomethine and phenolate stretches in the spectra of *R,R*-{$H_2(Et)_2$saldach(^{n}Bu-Im$^+$-Cl$^-$)$_2$} **(4a)** and *R,R*-{$H_2(Et)_2$saldach(^{n}Bu-Im$^+$-PF$_6^-$)$_2$} **(4b)** due to chelation with Pd(II) ions in {Pd(II)$(Et)_2$saldach(^{n}Bu-Im$^+$-Cl$^-$)$_2$} **(5a)** and {Pd(II)$(Et)_2$saldach(^{n}Bu-Im$^+$-PF$_6^-$)$_2$} **(5b).**

contribution of bis-(enol-imine) tautomer (see Scheme 2) could be confirmed from the notice of two singlets at δ 10.61 and 8.21 ppm (Fig. 3, left) characteristic for phenolic O-H and azomethinic protons, respectively, typical for bis-(enol-imine) tautomer. On the other hand, the minor contribution of enol-imine/phenolate-iminium tautomer could be detected from the observation of singlet at 10.50 ppm and a singlet/doublet set (8.42/8.39 ppm) characteristic for phenolic O-H and azomethinic (H–C═N–)/iminium (H-C═NH$^+$–) protons, respectively, for the typical enolimine/phenolate-iminium tautomer. Thus, from ^{1}H NMR spectrum of 4a we could highlight that, its central backbone is in the major enol-imine style with few contribution of the enol-imine/phenolate-iminium form (Scheme 2).

Contrary, examination of the ^{1}H NMR spectra of (4b,c) (see Fig. 3, left) revealed the following features; singlet peaks at ~9.20 (2H) and 8.43 (2H) ppm which are recognized as Ar-OH and azomethine (H-C═N) protons indicating that, their central saldach backbones are mainly in the neutral bis-(enol-imine) style.

At first glance for examination of ^{1}H NMR spectra of Pd(II) complexes it was noticed that a missing of phenolic proton peak along with an upfield shifting of the azomethinic proton signal ($\Delta\delta = \delta_{Pd(II)\ complex} - \delta_{free\ ligand} =$ ~0.05 ppm) (*cf.*Fig. 3, right) which is consistent with the deprotonation of phenolic-OH to form phenolate group coupled with the sharing of the phenolate oxygen and azomethinic nitrogen, as well, in chelation to the Pd(II) ions.

3.5. Pharmacology

The primary goal of our work is to find out a safe and cytotoxic Pd(II) saldach complexes used in mitigation of the inflammatory cytokine and proto-oncogene protein specific for the breast cancer tumors such as TNF alpha and Her2/neu. The secondary goal of this work is to evaluate the *in vitro* induced immune responses through apoptotic mechanisms of P53. The novel prepared complex revealed their ability to augment cell killing mechanisms of breast

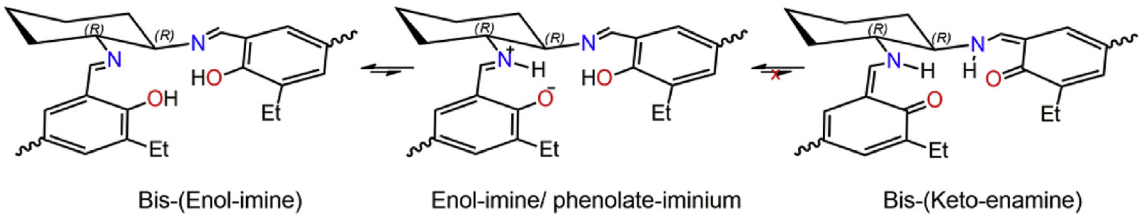

Scheme 2. Possible tautomeric forms in the parent saldach ligands.

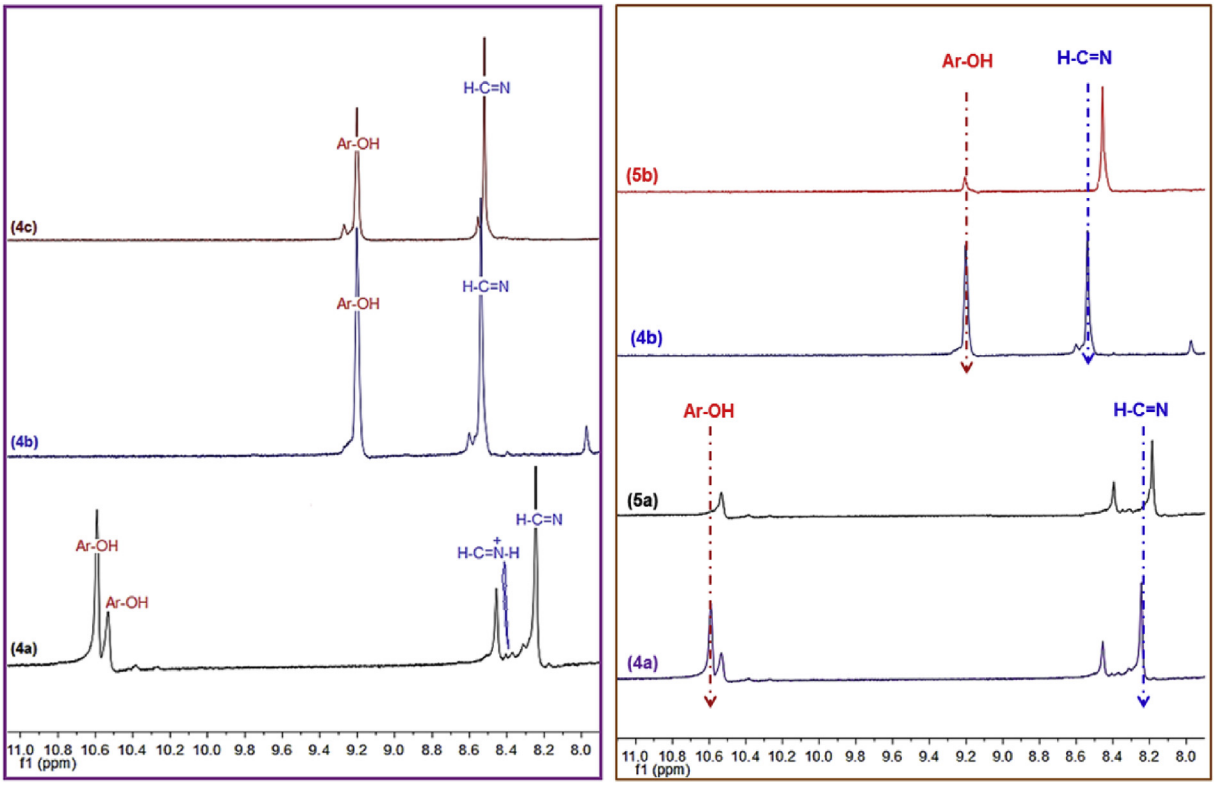

Fig. 3. Picked ^{1}H NMR segment (8.7–11.0 ppm), for comparison of the azomethine and phenolic protons resonance and their splitting profile in (left) the parent saldach ligands (4a,b) and (right) their Pd(II) complexes (5a,b).

cancer targeting downregulation of HER2/neu-specific manner and reduction of the inflammatory triggering mechanisms.

3.5.1. *In vitro* cytotoxicity

The new saldach ligands and their *cis*-Pd(II) complexes have been assessed for their *in vitro* cytotoxicity in comparison with Doxorubicin ($C_{27}H_{29}NO_{11}$, 543.52 g/mol), against human breast carcinoma (MCF-7) cell lines. The MCF-7 cells viability measurement (Fig. 4) demonstrated that all compounds have the ability to inhibit the growth of MCF-7 cells or inducing their death in a different activities profile. For instance, the *cis*-Pd(II) complexes (IC_{50} values = 0.010 ± 0.0001 to 0.035 ± 0.0003 μM) have the stronger growth-inhibitory effect than the native saldach ligands (IC_{50} values = 0.027 ± 0.0003 to > 0.054 μM). The overall activity is following an efficacy-pattern of 5a > 5c > 4a > 5b > 4c > 4b.

Based on these data, the specific molecular structure and the nature of the counter anion may play critical roles in the cytotoxicity effect of these compounds. Meanwhile, Pd(II) complex (5a) anchored bis-(imidazolium) chloride (5a) (IC_{50} = 0.010 ± 0.0001 μM) is the most effective in induction of MCF-7 cells death in comparison to the corresponding tetrafluoroborate (5c) or hexafluorophosphate (5b) analogues (IC_{50} = 0.025 ± 0.0003, 0.035 ± 0.0003 μM, respectively).

Interestingly, earlier studies regarding the mode of cytotoxic action of IL suggest that imidazolium ILs may induce oxidative stress, DNA deterioration, mitochondrial failure, and apoptosis in both malignant and normal cells [30,31]. Meanwhile, lipophilicity, cation-anion interactions, sensitivity to hydrolytic cleavage and bioavailability may act as the key structural features resulting in the anion-dependent cytotoxicity. Where the earlier theoretical study on imidazolium ILs revealed that small inorganic anions such as chloride ($[Cl]^{-}$) and tetrafluoroborate ($[BF_4]^{-}$) anions could be strongly interacted with water molecules than the bulky hydrophobic anion hexafluorophosphate ($[PF_6]^{-}$) [32]. Accordingly, the chloride and tetrafluoroborate salts can form direct stable ion pairs in aqueous media resulting in an enhanced bioavailability of thier corresponding ionic liquids, amplifying membrane interactions and inducing stronger cytotoxic effect.

Moreover, the hydrophobic substituent, ethyl group, at the ortho-position of the phenolic moieties and butyl at N-1 of imidazolium compartments have greatly enhanced the lipophilicity of the molecule and the cytotoxicity effect [33].

Additionally, the higher cytotoxicity of Pd(II) complexes as

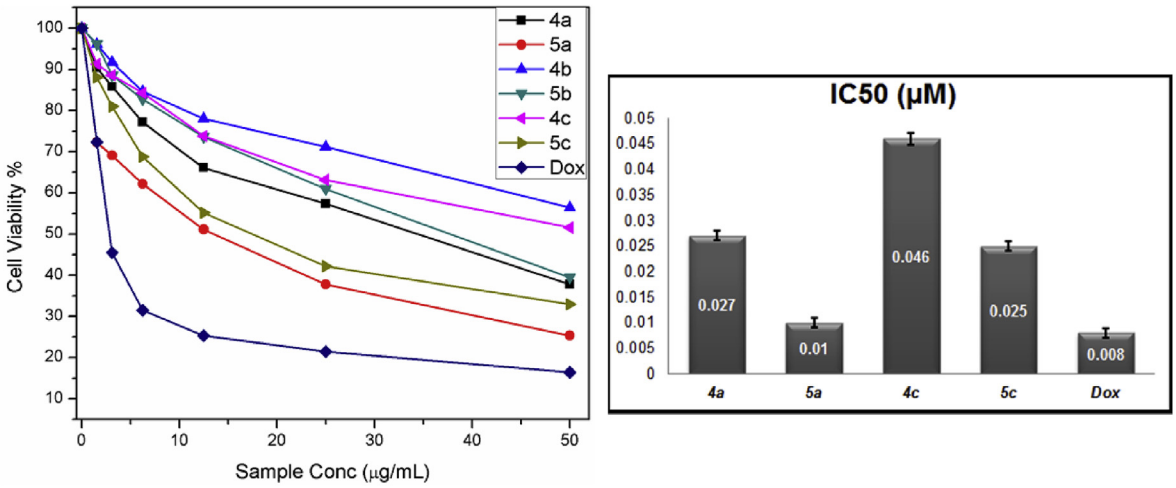

Fig. 4. Concentration-cytotoxic effects correlation and IC_{50} (μM) for the free ligand and their *cis*-Pd(II) complexes against the human MCF-7 cells.

compared to the native ligands could be ascribed to the square planar geometry of the *cis*-Pd(II) complexes which enable them to easily interact with the secondary structure of DNA nucleotides preventing DNA replication [34]. Our results were in agreement with Quiroga et al. who reported that the antitumor action of Pd(II) complexes is through their activity in suppression of ribonucleotide reductase inducing genetic material damage [24a].

3.5.2. DNA-binding studies

3.5.2.1. UV–vis stdiues. The interaction of CT-DNA with the most potent anticancer agent {Pd(Et)$_2$saldach(^{n}Bu-Im$^+$-Cl$^-$)$_2$} (5a) and its parent ligand {H$_2$(Et)$_2$saldach(^{n}Bu-Im$^+$-Cl$^-$)$_2$} (4a) were examined using spectrophotometric titration technique. The π→π* transition of the free ligand centered at 289 nm has been used for its spectrophotometric titration with CT-DNA under the physiological parameters (Fig. 5, left). As shown in Fig. 5 (left) a gradual increase in the concentrations of CT-DNA causing a significant hypochromic shift (Hyp% = 58%) along with a blue-shift of 5 nm in the π→π* transition. This π→π* transition peak fluctuation confirms the binding of the parent ligand (4a) to CT-DNA. Although the UV spectroscopic titration cannot determine the exact Ligand/CT-DNA binding mode, nevertheless, the hypochromism of π→π* transition peak may offer an evidence of partial insertion of the imidazolium rings into the ds-DNA and binding to the double-stranded DNA (ds-DNA) *via* a groove mode style [35].

Interestingly, the intrinsic binding constant, *K*b, for ligand 4a and complex 5a with CT-DNA could be calculated from Eq (1) [36];

$$\frac{[DNA]}{(\varepsilon_a - \varepsilon_f)} = \frac{[DNA]}{(\varepsilon_b - \varepsilon_f)} + \frac{1}{K_b(\varepsilon_b - \varepsilon_f)} \quad (1)$$

where, ε_a, ε_b, and ε_f are the extinction coefficients for the apparent, bound and free 4a or 5a at 289 and 291 nm, respectively. Meanwhile, ε_f was calculated from the calibration curve for 4a and 5a, separately, in their aqueous solution, following Beer's law. On the other hand, the apparent extinction coefficient, ε_a, was recognized as the observed absorbance (A_{obs})/concentration ratio (*i.e* A_{obs}/[4a or 5a]). The slope of a plot of [DNA]/($\varepsilon_a - \varepsilon_f$) vs. [DNA] assigned as a $1/(\varepsilon_b - \varepsilon_f)$ while a y-intercept is $1/K_b(\varepsilon_b - \varepsilon_f)$. So, K_b is the ratio slope/y-intercept (inset in Fig. 5). The calculated K_b values for 4a and 5a were found to be $(1.3 \pm 0.07) \times 10^5\ M^{-1}$ and $(3.6 \pm 1.1) \times 10^5\ M^{-1}$, respectively. These calculated K_b values for 4a and 5a suggest that 5a has significantly interacted with CT-DNA more than its native ligand, 4a.

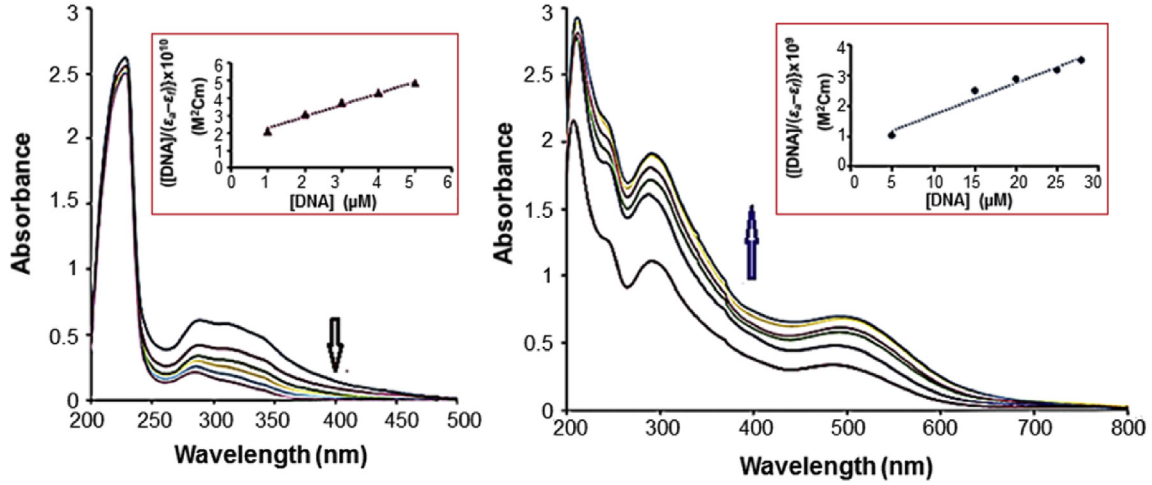

Fig. 5. UV spectroscopic titration of {H$_2$(Et)$_2$saldach(^{n}Bu-Im$^+$-X$^-$)$_2$} (4a) (6×10^{-5} M) (left) and its Pd(II) complex, {Pd(Et)$_2$saldach(^{n}Bu-Im$^+$-X$^-$)$_2$} (5a), (1×10^{-4} M) (right) with CT-DNA ((left) [DNA] = 0–5 mM (right) [DNA] = 0–28 mM. The arrows show peak intensity fluctuation with increasing [CT-DNA]. Inset: A plot of [DNA]/($\varepsilon_a - \varepsilon_f$) versus [DNA].

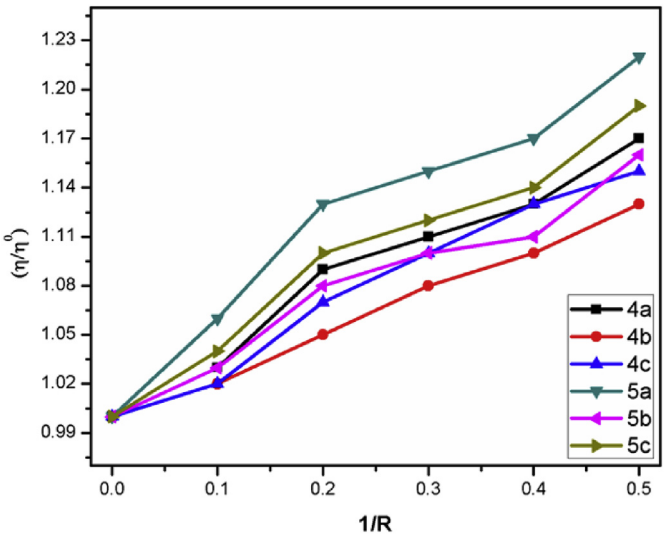

Fig. 6. Effect of free ligands (4a-c) or Pd(II) complexes (5a-c) on the viscosity of CT-DNA solution (1/R = [Compound]/[CT-DNA]).

3.5.2.2. Viscosity studies. The significant correlation between the relative viscosity (η/η^0) of DNA and the changes in length of DNA helix make the viscosity offers a clear insight about the extent and mode of interaction of DNA with different molecules. Where the intercalative interaction betweenthe stacked DNA's double helix and any foreign molecule results in increaining the gap between DNA base pairs and lengthening of the helix, as a result, the relative viscosity increases [28]. As noticed in Fig. 6, the relative viscosities of CT-DNA solution was increased by adding increasing amounts of free ligands (4a-c) or Pd(II) complexes (5a-c), with notable increasing for complexes more than free ligands. The results revealed that our new compound are bound to CT-DNA *via* the intercalation mode. Notworthy, The ability of the compounds to lengthen the DNA's double helix and cosesequently increases the viscosity of CT-DNA solution are in the order of: 5a > 5c > 4a > 5b > 4c > 4b.

Barton et al. [37], concluded that the main features of the substrate including molecular size, geometry, hydrophilicity/hydrophobicity, and hydrogen-bonding capacity play crucial roles in interaction with DNA. The ds-DNA has many terminal H-bonding acceptor/donor (HBA/HBD) sites belonged to the DNA nucleobases, it is quite possible that the HBA sites (N and O atoms of the azomethine, imidazolium, and phenolic groups) and HBD sites (H and C2-H atoms of the phenolic and imidazolium) (Fig. 7) of the free ligand (4a) could share in intermolecular H-bonding with the DNA nucleobases [38]. On the other hand, upon incremental additions of CT-DNA to the Pd(II) complex (5a), the intra-ligand electronic transition band for 5a centered at λ_{max} ~290 nm underwent a hypochromism up to 72% coupled with a blue-shift of 5 nm (Fig. 7, right) supporting the binding activity of the complex 5a to CT-DNA [39].

Moreover, the binding activity could be explained on the basis of the following aspects; (i) The presence of small hydrophilic anions $[Cl]^-$ which can easily departed from the Pd(II) complex allowing the double-charged cation, $[Pd(Et)_2saldach(^nBu\text{-}Im^+)_2]^{2+}$, to interact with the anionic phosphate backbone of CT-DNA electrostatically [40]. (ii) H-bonding association between the diverse HBA/HBD sites belonged to the complex and CT-DNA nucleobases. (iii) The *cis*-configuration of the Pd(II) complex enhances the π-π stacking and hydrophobic interactions between the aromatic fragments of complex-DNA nucleobases.

Interestingly, it was found that treatment of MCF-7 cells with *cis*-Pd(II) saldach complexes was significantly down-regulated the Her2/neu expression more than the free ligand and Doxorubicin with a P value of <0.05 as shown in Fig. 8. Meanwhile, the TNF displayed a high significant decrease and the apoptotic marker p53 showed significant up-regulation of in their expression in MCF-7 with $P < 0.01$ as shown in Fig. 8b.

Thus, the prepared complexes have triggered a down-regulation of TNF-α and considered as anti-TNF-α suppressing cell proliferation along with the inhibition of the Her2/neu and up-regulation of P53. Moreover, the current results were in contrast to some reports in the literature which had interpreted that inhibition of TNF-α has no influence on tumor cell growth, *in vitro* [41].

Evantaully, we could propse that the mode of antitumor action of *cis*-PdII) saldach complexes maybe through the modulation of the cytokine-dependent communication betweenthe tumor cells in its microenvironment. Furthermore, an important implication of these findings may be due to the significant growth inhibitory as a result of the ease of departure of small hydrophilic anions, $[Cl]^-$, from the$\{Pd(Et)_2saldach(^nBu\text{-}Im^+\text{-}Cl^-)_2\}$ (5a) allowing the free $[Pd(Et)_2saldach(^nBu\text{-}Im^+)_2]^{2+}$ cation to freely interact with the phosphate groups of DNA backbone through an electrostatic association and induced DNA damage. Whereas a more hydrophobic, bulkier anion ($[PF_6]^-$) may form an isolated film at the lipid/water boundary and diminish the bioavailability bis-imidazolium-saldach cation to a great extent. Additionally, Kacar et al. [42] reported that Pd(II) complexes can induce DNA double-stranded breaks. So, *cis*-Pd(II) saldach complexes considered as one of the most promising chemotherapeutic agents. Moreover, several lines of evidences have supported the effective role of HER2/neu overexpression in triggering the tumor pathogenesis and insufficient clinical course of treatment for human tumors. Furthermore, mice erbB2 (neu) overexpressed in transgenic mice accompanied with induced mammary tumors and enhancing tumorgenicity [43].

4. Conclusion

The present study had introduced an addition in the chemotherapy and preventive activity of some novel inhibitory

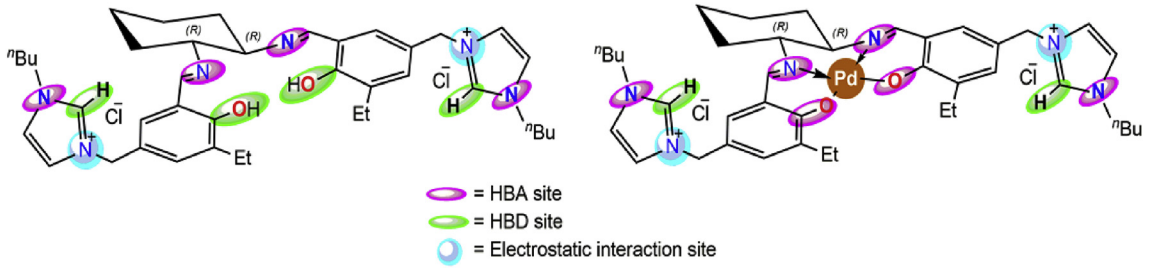

Fig. 7. All possible HBA sites (N and O atoms of the azomethine, imidazolium, and phenolic groups), HBD sites (H and C2-H atoms of the phenolic and imidazolium) and electrostatic interaction sites belonged to the $\{H_2(Et)_2saldach(^nBu\text{-}Im^+\text{-}X^-)_2\}$ (4a) and $\{Pd(Et)_2saldach(^nBu\text{-}Im^+\text{-}X^-)_2\}$ (5a) could share in binding to CT-DNA.

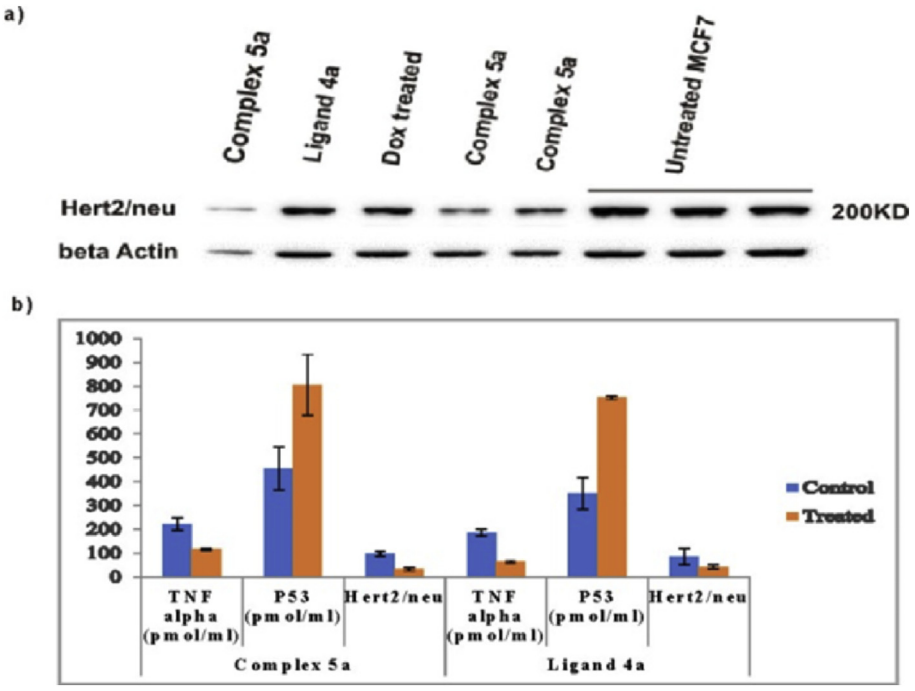

Fig. 8. Effect of ligand (4a) and saldsh complex (5a) against the reference drug DOx on the expression of Her2/neu a); b) quantitative estimation of the TNF-alpha signaling, P53, and densitometric expression of Her2/neu through the immunoblotting analysis in MCF-7 cell lines.

compounds for the differentiation and proliferation of the breast cancer cell. Based on the present research results, *cis*-palladium(II) complexes have been very successful in the inhibition of one of the proto-oncogenes HER2/neu related to the breast cancer proliferation parallel with the inflammatory mechanisms of TNFα and enhancing the apoptotic activity of P53. Additionally, the complex saldach palladium(II) and the counter anions have a specific molecular structure that may play critical roles in alleviation the cytotoxicity effect of these compounds. So, the newly saldach ligands and their *cis*-Pd(II) complexes have various inhibitory actions on breast cancer cells and considered as novel anticancer compounds.

On the basis of the promising findings presented in this paper, our future work will use the saldach complexes on different tumor cell lines and investigating their role on mitochondrial dynamic proteins activity and tumor progression.

Conflicts of interest

All authors contributed equally to the production of the manuscript and show no conflict of interest.

Appendix A. Supplementary data

Supplementary data to this article can be found online at https://doi.org/10.1016/j.molstruc.2019.04.119.

References

[1] a) L. Coussens, T.L. Yang-Feng, Y.C. Liao, E. Chen, A. Gray, J. McGrath, P.H. Seeburg, T.A. Libermann, J. Schlessinger, U. Francke, Tyrosine kinase receptor with extensive homology to EGF receptor shares chromosomal location with neu oncogene, Science 230 (1985) 1132–1139, https://doi.org/10.1126/science.2999974;
b) T. Akiyama, C. Sudo, H. Ogawara, K. Toyoshima, T. Yamamoto, The product of the human c-erbB-2 gene: a 185-kilodalton glycoprotein with tyrosine kinase activity, Science 232 (1986) 1644–1646, https://doi.org/10.1126/science.3012781.

[2] D.S. Salomon, R. Brandt, F. Ciardiello, N. Normanno, Epidermal growth factor-related peptides and their receptors in human malignancies, Crit. Rev. Oncol. Hematol. 19 (1995) 183–232. https://doi.org/10.1016/1040-8428(94)00144-I.

[3] a) D.J. Slamon, G.M. Clark, S.G. Wong, W.J. Levin, A. Ullrich, W.L. McGuire, Human breast cancer: correlation of relapse and survival with amplification of the HER-2/neu oncogene, Science 235 (1987) 177–182, https://doi.org/10.1126/science.3798106;
b) P.M. Ravdin, G.C. Chamness, The c-erbB-2 proto-oncogene as a prognostic and predictive marker in breast cancer: a paradigm for the development of other macromolecular markers-A review, Gene (Amst.) 159 (1995) 19–27. https://doi.org/10.1016/0378-1119(94)00866-Q;
(c) M.I. Lyu, M.G. Rosenblum, The immunocytokine scFv23/TNF sensitizes HER-2/neu–overexpressing SKBR-3 cells to tumor necrosis factor (TNF) via up-regulation of TNF receptor-1, Mol. Canc. Therapeut. 4 (2005) 1205–1213, https://doi.org/10.1158/1535-7163.MCT-05-0014.

[4] a) C.I. Bargman, M.C. Hung, R.A. Weinberg, The neu oncogene encodes an epidermal growth factor receptor-related protein, Nature 319 (1986) 226–230;
b) T. Yamamoto, S. Ikawa, T. Akiyama, Similarity of protein encoded by the human c-erb-B-2 gene to epidermal growth factor receptor, Nature 319 (1986) 230–234. https://doi.org/10.1038/319230a0.

[5] a) D.J. Slamon, W. Godolphin, L.A. Jones, Studies of the HER-2/neu proto-oncogene in human breast and ovarian cancer, Science 244 (1989) 707–712, https://doi.org/10.1126/science.2470152;
b) F.L. Tyson, C.M. Boyer, R. Kaufman, Expression and amplification of the HER-2/neu (c-erbB-2) protooncogene in epithelial ovarian tumors and cell lines, Am. J. Obstet. Gynecol. 165 (1991) 640–646. https://doi.org/10.1016/0002-9378(91)90300-G.

[6] a) M.C. Hung, Y.K. Lau, Semin. Basic science of HER-2/neu: a review, Semin. Oncol. 26 (1999) 51–59. PMID:10482194;
b) E. Tzahar, Y. Yarden, The ErbB-2/HER2 oncogenic receptor of adenocarcinomas: from orphanhood to multiple stromal ligands, Biochim. Biophys. Acta 1377 (1998), https://doi.org/10.1016/S0304-419X(97)00032-2. M25–37.

[7] A. Berchuck, A. Kamel, R. Whitaker, Overexpression of HER-2/neu is associated with poor survival in advanced epithelial ovarian cancer, Cancer Res. 50 (1990) 4087–4091.

[8] a) A. Lichtenstein, J.F. Gera, J. Andrews, J. Berenson, C.F. Ware, Inhibitors of ADP-ribose polymerase decrease the resistance of HER2/neu-expressing cancer cells to the cytotoxic effects of tumor necrosis factor, J. Immunol. 146 (1991) 2052–2058;
b) P. Tang, M.C. Hung, J. Klostergaard, TNF cytotoxicity: effects of HER-2/neu expression and inhibitors of ADP-ribosylation, Lymphokine Cytokine Res. 13 (1994) 117–123. PMID:7914750.

[9] a) A. Lichtenstein, J. Berenson, J.F. Gera, K. Waldburger, O. Martinez-Maza, J.S. Berek, Resistance of human ovarian cancer cells to tumor necrosis factor and lymphokine-activated killer cells: correlation with expression of HER2/neu oncogenes, Cancer Res. 50 (1990) 7364–7370;

b) R.M. Hudziak, G.D. Lewis, M.R. Shalaby, Amplified expression of the HER2/ERBB2 oncogene induces resistance to tumor necrosis factor alpha in NIH 3T3 cells, Proc. Natl. Acad. Sci. U.S.A. 85 (1988) 5102–5106. https://doi.org/10.1073/pnas.85.14.5102.

[10] a) K.R. Barnes, S.J. Lippard, Cisplatin and related anticancer drugs: recent advances and insights, Met. Ions Biol. Syst. 42 (2004) 143–177. PMID: 15206102;
b) B. Stordal, N. Pavlakis, R. Davey, Oxaliplatin for the treatment of cisplatin-resistant cancer: a systematic review, Cancer Treat Rev. 33 (2007) 347–357. https://doi.org/10.1016/j.ctrv.2007.01.009.

[11] a) J.L. Czlapinski, T.L. Sheppard, Nucleic acid template-directed assembly of Metallosalen– DNA conjugates, J. Am. Chem. Soc. 123 (2001) 8618–8619, https://doi.org/10.1021/ja0162212;
b) I. Ott, R. Gust, Non platinum metal complexes as anti-cancer drugs, Arch. Pharm. (Weinheim) 340 (2007) 117–126. https://doi.org/10.1002/ardp.200600151.

[12] a) G. Sava, S. Zorzet, C. Turrin, E. Vita, M. Soranzo, G. Zabucchi, M. Cocchietto, A. Bergamo, S. DiGiovine, G. Pezzoni, L. Sartor, S. Garbisa, Dual action of NAMI-A in inhibition of solid tumor metastasis: selective targeting of metastatic cells and binding to collagen, Clin. Cancer Res. 9 (2007) 1898–1905;
b) C.G. Hartinger, M.A. Jakupec, S. Zorbas-Seifried, M. Groessl, A. Egger, W. Berger, H. Zorbas, P.J. Dyson, B.K. Keppler, KP1019, a new redox-active anticancer agent–Preclinical development and results of a clinical phase I study in tumor patients, Chem. Biodivers. 5 (2008) 2140–2155. https://doi.org/10.1002/cbdv.200890195;
c) R. Gust, I. Ott, D. Posselt, K. Sommer, Development of cobalt (3, 4-diarylsalen) complexes as tumor therapeutics, J. Med. Chem. 47 (2004) 5837–5846, https://doi.org/10.1021/jm040763n.

[13] U. Ndagi, N. Mhlongo, M.E. Soliman, Metal complexes in cancer therapy – an update from drug design perspective, Drug Des. Dev. Ther. 11 (2017) 599–616, https://doi.org/10.2147/DDDT.S119488.

[14] a) A. Divsalar, A.A. Saboury, H. Mansoori-Torshizi, F. Ahmad, Design, synthesis, and biological evaluation of a new palladium(II) complex: β-lactoglobulin and K562 as targets, J. Phys. Chem. B 114 (2010) 3639–3647, https://doi.org/10.1021/jp909143b;
b) N.A. Al-Masoudi, B.H. Abdullah, A.H. Essa, R. Loddo, P. LaColla, Platinum and palladium-triazole complexes as highly potential antitumor agents, Arch. Pharm. (Weinheim) 343 (2010) 222–227. https://doi.org/10.1002/ardp.200900140;
c) G. Tamasi, M. Casolaro, A. Magnani, A. Sega, L. Chiasserini, L. Messori, C. Gabbiani, S.M. Valiahdi, M.A. Jakupec, B.K. Keppler, M.B. Hursthouse, R. Cini, New platinum–oxicam complexes as anti-cancer drugs. Synthesis, characterization, release studies from smart hydrogels, evaluation of reactivity with selected proteins and cytotoxic activity in vitro, J. Inorg. Biochem. 104 (2010) 799–814. https://doi.org/10.1016/j.jinorgbio.2010.03.010.

[15] a) E. Gao, C. Liu, M. Zhu, H. Lin, Q. Wu, L. Liu, Current development of Pd (II) complexes as potential antitumor agents, Anti Cancer Agents Med. Chem. 9 (2009) 356–368;
b) E.J. Gao, L. Wang, M.C. Zhu, L. Liu, W.Z. Zhang, Synthesis, characterization, interaction with DNA and cytotoxicity in vitro of the complexes [M(dmphen)(CO_3)]·H_2O [M=Pt(II), Pd(II)], Eur. J. Med. Chem. 45 (2010) 311–316. https://doi.org/10.1016/j.ejmech.2009.10.014.

[16] a) A.R. Kapdi, I.J.S. Fairlamb, Anti-cancer palladium complexes: a focus on PdX 2 L 2, palladacycles and related complexes, Chem. Soc. Rev. 43 (2014) 4751–4777;
b) M.D. Coskun, F. Ari, A.Y. Oral, M. Sarimahmut, H.M. Kutlu, V.T. Yilmaz, E. Ulukaya, Promising anti-growth effects of palladium(II) saccharinate complex of terpyridine by inducing apoptosis on transformed fibroblasts in vitro, Bioorg. Med. Chem. 21 (2013) 4698–4705, https://doi.org/10.1039/C4CS00063C.

[17] F. Darabi, H. Hadadzadeh, J. Simpson, A. Shahpiri, A water-soluble Pd(II) complex with a terpyridine ligand: experimental and molecular modeling studies of the interaction with DNA and BSA; and in vitro cytotoxicity investigations against five human cancer cell lines, New J. Chem. 40 (2016) 9081–9097, https://doi.org/10.1039/C6NJ01880G.

[18] L. Tusek-Bozic, A. Furlani, V. Scarcia, E. De Clercq, J. Balzarini, Spectroscopic and biological properties of palladium (II) complexes of ethyl 2-quinolylmethylphosphonate, J. Inorg. Biochem. 72 (1998) 201–210. https://doi.org/10.1016/S0162-0134(98)10081-8.

[19] a) S. Bhattacharya, S.S. Mandal, DNA cleavage by intercalatable cobalt–bispicolylamine complexes activated by visible light, Chem. Commun. (1996) 1515–1516, https://doi.org/10.1039/CC9960001515;
b) S.E. Rokita, C.J. Burrows, Salen-metal complexes, in: Small Molecule DNA and RNA Binders, vol. 1, Wiley-VCH, 2003;
c) H.Y. Shrivastava, S.N. Devaraj, B.U. Nair, A Schiff base complex of chromium(III): an efficient inhibitor for the pathogenic and invasive potential of Shigella dysenteriae, J. Inorg. Biochem. 98 (2004) 387–392. https://doi.org/10.1016/j.jinorgbio.2003.11.012.

[20] J.G. Muller, L.A. Kayser, S.J. Paikoff, V. Duarte, N. Tang, R.J. Perez, S.E. Rokita, C.J. Burrows, Formation of DNA adducts using nickel (II) complexes of redox-active ligands: a comparison of salen and peptide complexes, Coord. Chem. Rev. 185–186 (1999) 761–774. https://doi.org/10.1016/S0010-8545(99)00043-0.

[21] J. Haribabu, M.M. Tamizh, C. Balachandran, Y. Arun, N.S.P. Bhuvanesh, A. Endo, R. Karvembu, Synthesis, structures and mechanistic pathways of anticancer activity of palladium(II) complexes with indole-3-carbaldehyde thiosemicarbazones, New J. Chem. 42 (2018) 10818–10832, https://doi.org/10.1039/C7NJ03743K.

[22] V. Rajendiran, M. Palaniandavar, V.S. Periasamy, M.A. Akbarsha, Supramolecular interaction of transition metal complexes with albumins and DNA: spectroscopic methods of estimation of binding parameters, J. Inorg. Biochem. 116 (2012) 151–162. https://doi.org/10.1002/aoc.4150.

[23] a) M. Morshedi, H. Hadadzadeh, Mononuclear Co(III) and Ni(II) complexes with polypyridyl ligands, $[Co(phen)_2(taptp)]^{3+}$ and $[Ni(phen)_2(taptp)]^{2+}$: synthesis, photocleavage and DNA-binding, J. Fluoresc. 23 (2013) 247–259. https://doi.org/10.1007/s10895-012-1143-0;
b) K.J. Du, J.Q. Wang, J.F. Kou, G.Y. Li, L.L. Wang, H. Chao, L.N. Ji, DNA-binding and topoisomerase inhibitory activity of ruthenium(II) polypyridyl complexes, Eur. J. Med. Chem. 46 (2011) 1056–1065. https://doi.org/10.1016/j.ejmech.2011.01.019.

[24] a) A.G. Quiroga, J.M. Pérez, I. López-Solera, J.R. Masaguer, A. Luque, P. Román, A. Edwards, C. Alonso, C. Navarro-Ranninger, Novel tetranuclear orthometalated complexes of Pd(II) and Pt(II) derived from p-isopropylbenzaldehyde thiosemicarbazone with cytotoxic activity in cis-DDP resistant tumour cell lines. Interaction of these complexes with DNA, J. Med. Chem. 41 (1998) 1399–1408, https://doi.org/10.1021/jm970520d;
b) H.F.G. Barbosa, M. Attjioui, A.P.G. Ferreira, E.R. Dockal, N.-E. El Gueddari, B.M. Moerschbacher, É.T.G. Cavalheiro, Synthesis, characterization and biological activities of biopolymeric Schiff bases prepared with chitosan and salicylaldehydes and their Pd(II) and Pt(II) complexes, Molecules 22 (2017) 1987–2006, https://doi.org/10.3390/molecules22111987.

[25] J. Toneatto, P.F. Garcia, G.A. Argüello, Advances on the interaction of polypyridyl Cr(III) complexes with transporting proteins and its potential relevance in photodynamic therapy, J. Inorg. Biochem. 105 (2011) 1299–1305. https://doi.org/10.1016/j.jinorgbio.2011.07.013.

[26] K.S. Egorova, E.G. Gordeev, V.P. Ananikov, Biological activity of ionic liquids and their application in pharmaceutics and medicine, Chem. Rev. 117 (2017) 7132–7189, https://doi.org/10.1021/acs.chemrev.6b00562.

[27] a) R.F.M. Elshaarawy, C. Janiak, Toward new classes of potent antibiotics: synthesis and antimicrobial activity of novel metallosaldach–imidazolium salts, Eur. J. Med. Chem. 75 (2014) 31–42. https://doi.org/10.1016/j.ejmech.2013.09.029;
b) R.F.M. Elshaarawy, C. Janiak, Ionic liquid-supported chiral saldach with tunable hydrogen bonding: synthesis, metalation with Fe(III) and in vitro antimicrobial susceptibility, Tetrahedron 70 (43) (2014) 8023–8032. https://doi.org/10.1016/j.tet.2014.08.034;
c) R.F.M. Elshaarawy, T.B. Mostafa, A.A. Refaee, E.A. El-Sawi, Ionic Sal-SG Schiff bases as new synergetic chemotherapeutic candidates: synthesis, metalation with Pd(II) and in vitro pharmacological evaluation, RSC Adv. 5 (2015) 68260–68269, https://doi.org/10.1039/C5RA11083A.

[28] T. Mosmann, Rapid colorimetric assay for cellular growth and survival: application to proliferation and cytotoxicity assays, J. Immunol. Methods 65 (1983) 55–63. https://doi.org/10.1016/0022-1759(83)90303-4.

[29] G. Kalaiarasi, H.R. Jain, S. Puschman, K.P. Chandrika, R.P. Preethi, New binuclear Ni(II) metallates containing ONS chelators: synthesis, characterisation, DNA binding, DNA cleavage, protein binding, antioxidant activity, antimicrobial and *in vitro* cytotoxicity, New J. Chem. 41 (2017) 2543–2560, https://doi.org/10.1039/c6nj03516g.

[30] a) X.Y. Li, C.Q. Jing, W.L. Lei, J. Li, J. Wang, Apoptosis caused by imidazolium-based ionic liquids in PC12 cells, J. Ecotoxicol. Environ. Saf. 83 (2012) 102–107. https://doi.org/10.1016/j.ecoenv.2012.06.013;
b) S.V. Malhotra, V. Kumar, C. Velez, B. Zayas, Imidazolium-derived ionic salts induce inhibition of cancerous cell growth through apoptosis, MedChemComm 5 (2014) 1404–1409, https://doi.org/10.1039/C4MD00161C.

[31] K.S. Egorova, E.G. Gordeev, V.P. Ananikov, Biological activity of ionic liquids and their application in pharmaceutics and medicine, Chem. Rev. 117 (10) (2017) 7132–7189, https://doi.org/10.1021/acs.chemrev.6b00562.

[32] J. Dupont, T. Itoh, P. Lozano, S.V. Malhotra, Environmentally Friendly Syntheses Using Ionic Liquids, CRC Press, Boca Raton-London-New York, 2015.

[33] N. Berthet, V. Martel-Frachet, F. Michel, C. Philouze, S. Hamman, X. Ronotb, F. Thomas, Nuclease and anti-proliferative activities of copper(II) complexes of N_3O tripodal ligands involving a sterically hindered phenolate, Dalton Trans. 42 (2013) 8468–8483, https://doi.org/10.1039/C3DT32659D.

[34] P. Kavitha, K.L. Reddy, Synthesis, spectral characterisation, morphology, biological activity and DNA cleavage studies of metal complexes with chromone Schiff base, Arab. J. Chem. 9 (2016) 596–605. https://doi.org/10.1016/j.arabjc.2012.09.001.

[35] F. Dimiza, S. Fountoulaki, A.N. Papadopoulos, C. Kontogiorgis, V. Tangoulis, C.P. Raptopoulou, V. Psycharis, A. Terzis, D.P. Kessissoglou, G. Psomas, Non-steroidal antiinflammatory drug–copper(II) complexes: structure and biological perspectives, Dalton Trans. 40 (2011) 8555–8568, https://doi.org/10.1039/C1DT10714C.

[36] A. Wolfe, G.H. Shimer, T. Meehan, Polycyclic aromatic hydrocarbons physically intercalate into duplex regions of denatured DNA, Biochemistry 26 (1987) 6392–6396, https://doi.org/10.1021/bi00394a013.

[37] J.K. Barton, J.M. Goldberg, C.V. Kumar, N.J. Turro, Binding modes and base specificity of tris(phenanthroline)-ruthenium(II) enantiomers with nucleic acids: tuning the stereoselectivity, J. Am. Chem. Soc. 108 (1989) 2081–2088, https://doi.org/10.1021/ja00268a057.

[38] A.M. Pyle, J.P. Rehmann, R. Meshoyrer, C.V. Kumar, N.J. Turro, J.K. Barton,

Mixed-ligand complexes of ruthenium(II): factors governing binding to DNA, J. Am. Chem. Soc. 111 (1989) 3051–3058, https://doi.org/10.1021/ja00190a046.

[39] G. Kalaiarasi, G. Aswini, S.R.J. Rajkumar, S. Dharani, V.M. Lynch, R. Prabhakaran, Synthesis, spectral, structural characterization and biological activity of new palladium(II) complexes containing 3-acetyl-8-methoxy-2H-chromen-2-one derived Schiff bases, Appl. Organomet. Chem. (2018) e4466–e4481. https://doi.org/10.1002/aoc.4466.

[40] F. Arjmand, I. Yousuf, Y. Zaidi, L. Toupet, Crystal structure determination, spectroscopic characterization and biological profile of a tailored ionic molecular entity, Sn(IV) iminodiacetic acid–piperazinediium conjugate: *in vitro* DNA/RNA binding studies, Topo I inhibition activity, cytotoxic and systemic toxicity studies, RSC Adv. 5 (2015) 16250–16264, https://doi.org/10.1039/C4RA13718C.

[41] a) J.H. Egberts, V. Cloosters, A. Noack, B. Schniewind, L. Thon, S. Klose, B. Kettler, C. von Forstner, C. Kneitz, J. Tepel, D. Adam, H. Wajant, H. Kalthoff, A. Trauzold, Anti-tumor necrosis factor therapy inhibits pancreatic tumor growth and metastasis, Cancer Res. 68 (2008) 1443–1450, https://doi.org/10.1158/0008-5472.CAN-07-5704;
b) H. Kulbe, R. Thompson, J.L. Wilson, S. Robinson, T. Hagemann, R. Fatah, D. Gould, A. Ayhan, F. Balkwill, The inflammatory cytokine tumor necrosis factor-α generates an autocrine tumor-promoting network in epithelial ovarian cancer cells, Cancer Res. 67 (2007) 585–592, https://doi.org/10.1158/0008-5472.CAN-06-2941.

[42] O. Kacar, B. Cevatemre, I. Hatipoglu, N. Arda, E. Ulukaya, V.T. Yilmaz, C. Acilan, The role of cell cycle progression for the apoptosis of cancer cells induced by palladium(II)-saccharinate complexes of terpyridine, Bioorg. Med. Chem. 25 (6) (2017) 1770–1777. https://doi.org/10.1016/j.bmc.2017.01.033.

[43] Z. Mao, M. Bozzella, A. Seluanov, V. Gorbunova, DNA repair by nonhomologous end joining and homologous recombination during cell cycle in human cells, Cell Cycle 7 (2008) 2902–2906. https://doi.org/10.4161/cc.7.18.6679.